RSC Advances

PAPER

View Article Online
View Journal | View Issue

Cite this: *RSC Adv.*, 2021, **11**, 7251

Azo synthesis meets molecular iodine catalysis†

Rozhin Rowshanpour and Travis Dudding *

A metal-free synthetic protocol for azo compound formation by the direct oxidation of hydrazine HN–NH bonds to azo group functionality catalyzed by molecular iodine is disclosed. The strengths of this reactivity include rapid reaction times, low catalyst loadings, use of ambient dioxygen as a stoichiometric oxidant, and ease of experimental set-up and azo product isolation. Mechanistic studies and density functional theory computations offering insight into this reactivity, as well as the events leading to azo group formation are presented. Collectively, this study expands the potential of main-group element iodine as an inexpensive catalyst, while delivering a useful transformation for forming azo compounds.

Received 15th January 2021
Accepted 2nd February 2021

DOI: 10.1039/d1ra00369k

rsc.li/rsc-advances

Introduction

Azo compounds have captivated chemists ever since their debut in the 1860's and use as an industrial manufactured color, shortly after Peter Griess's synthesis of Manchester Bismarck brown.[1] Nowadays, the commercial, academic and industrial uses of azo compounds are widespread, including applications as organic dyes and pigments,[2] free-radical initiators,[3] acid–base indicators[4] and chemosensors.[5] Beyond this mélange of usages, the switchable and spatiotemporal (light/thermal)-driven control of *E- vs. Z*-azo group double geometry of many azo compounds continues to prompt their use in photoresponsive soft materials functioning as liquid crystals,[6] smart polymers,[7] photochromic ligands for optochemical genetics[8] and photoswitches.[9]

As to be expected, this revered status has ushered in the advancement of various synthetic strategies for accessing (hetero)aryl functionalized azo compounds, yet practical synthetic methods for preparing these valuable compounds is needed. Among the most widely used methods for forming azo compounds are oxidative dimerization of aromatic amines,[10] reductive dimerization of nitrobenzenes,[11] Mills reaction,[12] diazonium coupling[13] and oxidative dehydrogenation[14] (Fig. 1, top); however, each of these synthetic methods have inherent drawbacks, such as employing toxic and expensive transition metals and/or hazardous reagents. For instance, the oxidative dimerization of aromatic amines frequently relies on the use of stoichiometric AgO,[15] ferrate salts,[16] *tert*-butyl hypoiodite[17] or environmentally unfriendly heavy-metal oxidants $BaMnO_4$,[18] $Pb(OAc)_4$,[19] and HgO.[20] Moreover, the Mills reaction[12] and diazonium coupling[13] require the use of toxic nitrosoarenes or explosive diazonium salt substrates. Similarly, reductive dimerization of nitroarenes[11] is plagued by the use of toxic and often carcinogenic nitro-containing compounds.

From this precedent along with other works,[21,22] and with it, a heavy reliance upon transition metals and/or hazardous reagents, the prospect of employing the oxidative capacity of main-group elements for azo group construction captured our attention. This possibility was especially appealing in light of a growing interest in replacing, or at the very least, complementing metal-based procedures with sustainable main group element-catalyzed protocols.[23] Driving this interest, the key parameters of cost, dwindling supplies of precious metals and associated political factors, and importantly global sustainability enabling productive harmony, stability and resilience to support present and future generations. Towards this end, we report herein the first metal-free, synthetic protocol for azo compound

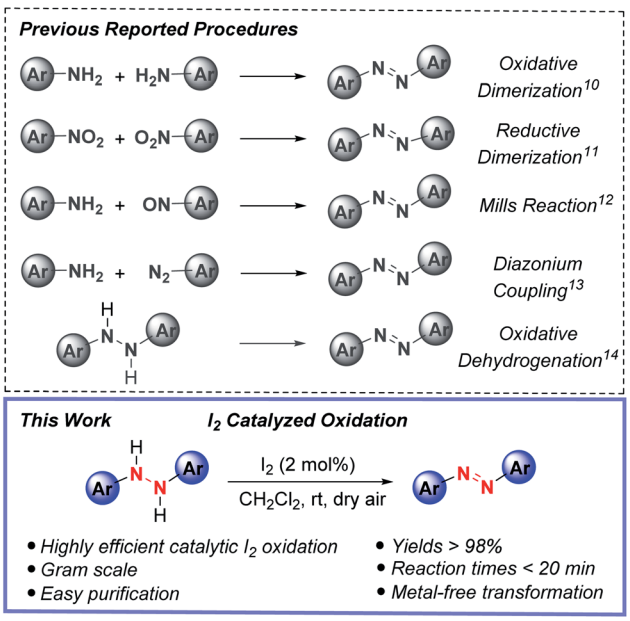

Fig. 1 Previous reported procedures for azo synthesis (top) and current iodine catalyzed synthesis of azo compounds (bottom).[10–14]

Brock University, 1812 Sir Isaac Brock Way, St. Catharines, Ontario, L2S 3A1, Canada. E-mail: tdudding@brocku.ca

† Electronic supplementary information (ESI) available. See DOI: 10.1039/d1ra00369k

formation by the direct oxidation of hydrazine HN–NH bonds to azo group functionality catalyzed by substoichiometric amounts of molecular iodine (Fig. 1, bottom). The strengths of this reactivity include rapid reaction times, low catalyst loadings, use of ambient dioxygen as a stoichiometric oxidant, and ease of experimental set-up and azo product isolation.

Results and discussion

At the outset of this study with an eye towards using easy-to-handle, environmentally friendly and relatively inexpensive solid molecular iodine (*e.g.*, over the last 5 years the bulk price of iodine has been $19–27 per kg) as a catalyst for azo double bond formation, we sought to delineate to what degree, if any, halogen bonding might have in triggering hydrazine HN–NH bond oxidation. Prompting this interest, among other factors, was the prominence of iodine-catalyzed reactions, many of which catalytically pivot around the formation of a "halogen bond" (X–B)—defined by IUPAC as the association between the electrophilic region of a polarized halogen atom and a Lewis basic unit.[24] The electrophilic region, in this case, commonly being referred to as a sigma hole (σ).[25] For molecular iodine this feature is clearly visible from the calculated electrostatic potential surface, displaying significant anisotropic electron distribution with positive polarization on the iodine atoms (Fig. 2, left-hand side, top).

With this bearing in mind, and in reflecting upon the history of the halogen bond dating back more than two-centuries to the first reported synthesis of a halogen bond complex $NH_3\cdots I_2$ by Colin in 1814,[26] it occurred to us that the formation of a hydrazine–I_2 complex should be a facile process. Indeed, formation of computed n-type halogen bond complex **XB** from diphenyl hydrazine and I_2 was computed to be exergonic by −0.1 kcal mol^{-1} at the (IEFPCM$_{DCM}$)UAPFD/def2-TZVP//UAPFD/DGDZVP level of theory. This complex displayed an almost linear N···I–I angle of 175.9° with nitrogen-iodine and iodine–iodine bond distances of 2.77 Å and 2.76 Å (Fig. 2, bottom left-hand side). Moreover, in foreshadowing reactivity, the highest occupied molecular orbital (HOMO, −0.26 eV) of this halogen bond complex was localized upon the hydrazine fragment, while the lowest unoccupied molecular orbital (LUMO, −0.09 eV), dominated by anti-bonding σ*-character, resided on I_2 (Fig. 2, middle and right-hand side).

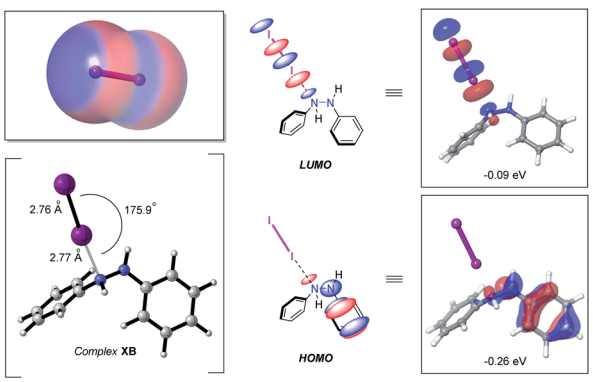

Fig. 2 Electrostatic potential surface of I_2 (electronegative (red) and electropositive (blue) regions (left-hand side, top)) computed at the B3LYP-D3/lacv3p**++ level of theory (isovalue = −0.003 (max = 0.3, min = −0.3)). Halogen bond complex **XB** (left-hand side, bottom) computed at the (IEFPCM$_{DCM}$)UAPFD/def2-TZVP//UAPFD/DGDZVP level of theory. Chemdraw and computed HOMO and LUMO of complex **XB** with orbital energies in eV (middle and right-hand side).

Optimization studies

With this insight, yet cautiously aware of the lack of a reported metal-free molecular iodine-catalyzed oxidation of hydrazine HN–NH bonds to azo N=N double bonds,[27] we commenced our study by investigating the reaction of diphenyl hydrazine (**1a**) in various solvents using catalytic iodine loadings (2–10 mol%) as summarized in Table 1. To this end, performing the reaction with a tenth of an equivalent of molecular iodine at room temperature in the presence of light and dry air as a stoichiometric co-oxidant resulted in very little azo product (**2a**) formation in polar protic solvent MeOH (Table 1, entry 1). Further, nonpolar solvents hexane and toluene proved even worse (Table 1, entries 2 and 3), whereas polar aprotic solvents, including acetone, acetonitrile, ethyl acetate, and tetrahydrofuran (THF) resulted in negligible conversions (Table 1, entries 4–7). Suspecting this poor reactivity was not a systemic problem, but rather an intrinsic feature of (1) hydroxyl, nitrile or carbonyl binding to I_2, that is, a solvent–solute sequestering effect or (2) insolubility of I_2 in nonpolar solvents, we performed the reaction in dichloromethane (DCM) and chloroform ($CHCl_3$). The logic for choosing these solvents stemming from their weak ability to engage in halogen–halogen or hydrogen-halogen bonding with iodine, while offering good solubility. Indeed,

Table 1 Screening iodine-catalyzed oxidation conditions for azobenzene formation[a]

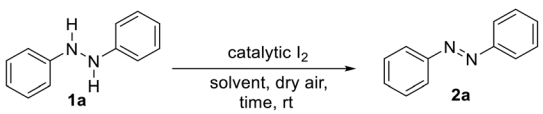

Entry	Solvent	Catalyst loading	Reaction conditions	Reaction time	Yield[b] (%)
1	MeOH	10 mol%	Room light	2 hours	>5
2	Toluene	10 mol%	Room light	2 hours	0
3	Hexane	10 mol%	Room light	2 hours	0
4	Acetone	10 mol%	Room light	2 hours	0
5	Acetonitrile	10 mol%	Room light	2 hours	0
6	Ethyl acetate	10 mol%	Room light	2 hours	0
7	Dry THF	10 mol%	Room light	2 hours	>5
8	Dry DCM	10 mol%	Room light	1 hour	100
9	Dry chloroform	10 mol%	Room light	1 hour	92
10	Dry DCM	5 mol%	Room light	1 hour	100
11	Dry DCM	2 mol%	Room light	1 hour	100
12	**Dry DCM**	**2 mol%**	**Dark**	**20 min**	**100**
13	Dry DCM	—	Dark	48 hours	0

[a] Reaction conditions: **1a** (1 mmol), solvent (5.0 mL) and I_2 (2–10 mol%) at room temperature under a dry air atmosphere in the absence/presence of ambient light. [b] Yields are determined by quantitative ^{1}H NMR using $CDCl_3$ as the internal standard.

this hypothesis proved productive as full conversion to product azobenzene **2a** occurred in an hour with DCM as the solvent and high conversion was observed in $CHCl_3$ (Table 1, entries 8 and 9). Moreover, decreasing the loading of catalyst I_2 afforded high conversion (Table 1, entries 10 and 11). Meanwhile, the use of dry air in the absence of light dramatically reduced the reaction time (Table 1, entry 12). Lastly, demonstrating the importance of iodine as a catalyst, no conversion was observed in the absence of I_2 (Table 1, entry 13).

Substrate scope

With the optimal reaction conditions established, we briefly examined the scope of this azo-forming protocol. To this end, various 1,2-disubstituted hydrazines with electron-rich and electron-poor aromatic groups smoothly reacted to furnish the target azo compounds in good-to-excellent yields (**2a–u**, Table 2). For instance, the reaction of *o*- and/or *p*-alkyl substituted aryl hydrazines (**1a–i**) successfully afforded aromatic azo compounds **2a–i** in good-to-high yields, though sterically hindered hydrazines **1i** provided a slightly reduced yield of azo compound **2i**. Meanwhile, the presence of inductively-withdrawing and weak electron-donating *p*-substituted halogens on the hydrazine aryl rings had little effect on the reaction efficiency. For instance, *p*-iodo-, *p*-fluoro-, and *p*-chloro-substituted aryl hydrazines (**1j–l**) smoothly reacted to afford azo compounds **2j–l**. Similarly, *o-chloro*-substituted aryl hydrazine **1m** was compatible, furnishing azo compound **2m** in high yield. Moreover, *p*-Alkyl and *m*-chloro- or *m*- or *p*-bromo-substituted aryl hydrazines (**1n–p**) underwent efficient oxidation to provide azo compounds **2n–p**. Further, the presence of electron-withdrawing trifluoromethyl- and trifluoromethyl ether groups had no effect on the reaction with azo compounds **2q–s** formed in high yields. Likewise, the reaction of electron-donating *p*-methoxy-substituted aryl hydrazine **1t** afforded azo product **2t** in high yield. Nitro functionality was also tolerated with azo compound **2u** formed in high yield. Lastly, to demonstrate the synthetic utility of this methodology, we performed a gram-scale reaction using 2.15 grams of **1a** to afford **2a** in 94% isolated yield (Table 2, bottom).

Table 2 Table of substrates for iodine-catalyzed oxidation[a,b]

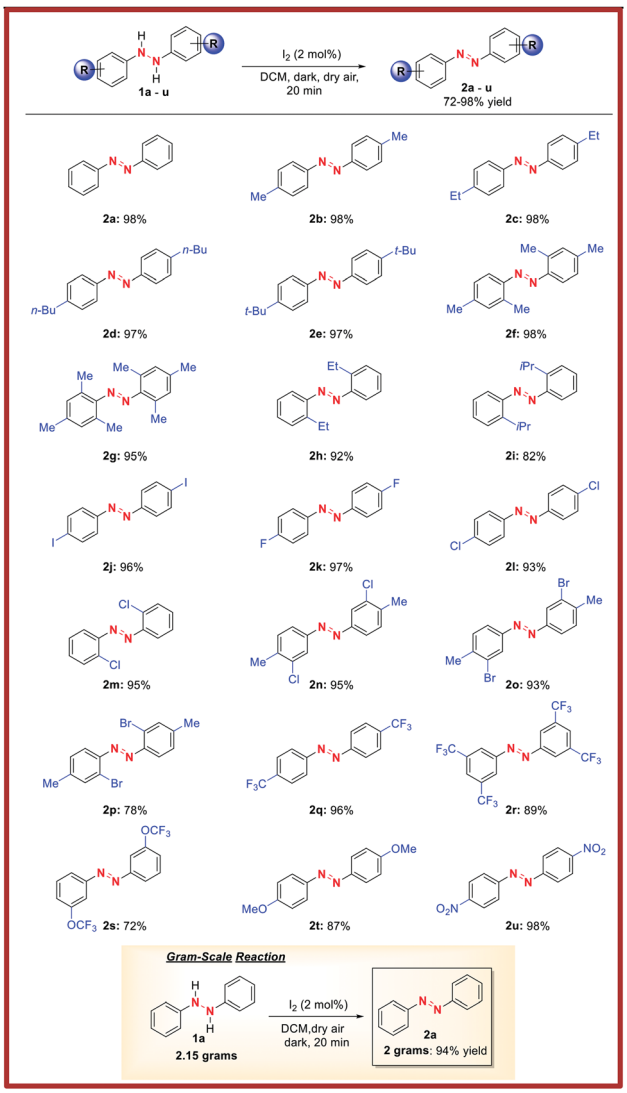

[a] Reactions conditions: **1a–u** (1 mmol), solvent (5.0 mL) and I_2 (2 mol%) at room temperature under a dry air atmosphere in the absence of light for 20 minutes. [b] Yields refer to the isolated material.

Control studies

Our interest next shifted to understanding the mechanistic details of this simple iodine-catalyzed azo N=N double bond forming reaction. An initial reaction using catalytic iodine (2 mol%) in the absence of air negatively affected azo product formation, suggesting the oxidation of molecular iodine or iodide ion to higher oxidation states might have a role in the reaction (Table 3, entry 1). To explore this aspect further, the role of higher iodine oxidation states were investigated using hydrogen peroxide (entry 2) resulting in quantitative conversion of **1a** to azobenzene (**2a**). Moreover, when we added DMSO (5 mol%, entry 3), a very good iodonium binding solvent,[23] to the original iodine (2 mol%) catalyzed reaction conditions, a good conversion was obtained, thus suggesting iodonium is not involved in the reaction. On the other hand, this finding is not at all surprising and can be explained by the fact that DMSO is known to oxidize iodine, thus implicating oxidative pathway(s). On the other hand, in the presence of 10 mol% KOH (entry 4), which could form potassium hypoiodite (KOI) *in situ*, no azo product was formed suggesting that a hypoiodous/hypoiodite pathway is unlikely.

Further, addition of radical scavenger 2,2,6,6-tetramethyl-1-piperidinyloxy (TEMPO) to the reaction had little effect, hinting that a radical pathway was not involved (entries 5 and 6).[28] Next, exchanging elemental iodine for HI still provided product suggesting that hydrogen iodide might be an intermediate in the reaction (entry 7). Conversely, the use of HCl resulted in no conversion establishing the essential role of iodine ion in this reaction (entry 8). Meanwhile, the addition of potassium iodide (10 mol%), negatively affected the reaction outcome (entry 9), which might be due to the formation of potassium triiodide. The use of molecular bromine instead iodine as a catalyst was

Table 3 Control studies of iodine-catalyzed oxidation[a]

Entry	Catalyst (2 mol%)	Additive	Conditions	Reaction time	Conversion[b] (%)
1	I_2	—	N_2, dark	2 hours	0
2	I_2	H_2O_2	Dry air, dark	20 min	100
3	I_2	DMSO (5 mol%)	Dry air, dark	20 min	100
4	I_2	KOH (10 mol%)	Dry air, dark	2 hours	0
5	I_2	TEMPO (5 mol%)	Dry air, dark	2 hours	74
6	I_2	TEMPO (100 mol%)	Dry air, dark	1 hour	100
7	—	HI (10 mol%)	Dry air, dark	20 min	100
8	—	HCl (10 mol%)	Dry air, dark	2 hours	0
9	—	KI (10 mol%)	Dry air, dark	2 hours	8
10	Br_2	—	Dry air, dark	2 hours	0
11	I_2	Water (5 mol%)	Dry air, dark	1 hour	40
12	I_2	Water (10 mol%)	Dry air, dark	1 hour	68

[a] Reaction conditions: **1a** (1 mmol), dry DCM (5.0 mL) and catalyst I_2 (2 mol%) in presence/absence of additives at room temperature, in the absence of light and under dry air atmosphere or $N_{2(g)}$. [b] Yields were determined by ^{1}H NMR.

also attempted resulting in no observed azo product formation and clearly demonstrating the importance of I_2 as a catalyst (entry 10). Lastly, moisture had a negative effect on reactivity, suggesting *in situ* derived hypoiodous acid (HOI) formed by disproportionation of molecular iodine and water had a negative effect on azo product formation (entries 11 and 12).

Mechanistic studies

As a last tool for understanding this reactivity we turned to DFT computations at the (IEFPCM$_{DCM}$)UAPFD/def2-TZVP//UAPFD/DGDZVP level of theory using diphenyl hydrazine as a representative substrate. Ultimately, this led to the tentative computed pathway depicted in Fig. 3 initiating from hydrazine **1a** that upon binding to I_2 forms halogen bond complex **XB**.

Next, following slight structural reorganization subsequent first-order saddle point **TS1** with a Gibbs free activation barrier ($\Delta G^{\ddagger}$) of 13.9 kcal mol^{-1} is surmounted. Defining this transition state involving Hydrogen Atom Transfer (HAT) and electron transfer type events were bond-breaking and bond-making distances of 1.44 Å and 1.81 Å. The resulting cationic azo intermediate **2a**-H$^+$ of **TS1** then reacts by proton transfer transition state **TS2** with an activation barrier of 19.9 kcal mol^{-1} and bond-breaking and bond-making distances of 1.67 Å and 1.93 Å. Desired azo product (**2a**) formation follows concomitant with the reaction of dioxygen and *in situ* derived HI to afford water and catalytic I_2. Collectively, these transformations result in an overall exergonic process of −34.9 kcal mol^{-1}. Meanwhile, in terms of the energetic span model and turnover frequency (TOF), halogen bond complex **XB** corresponds to the TOF

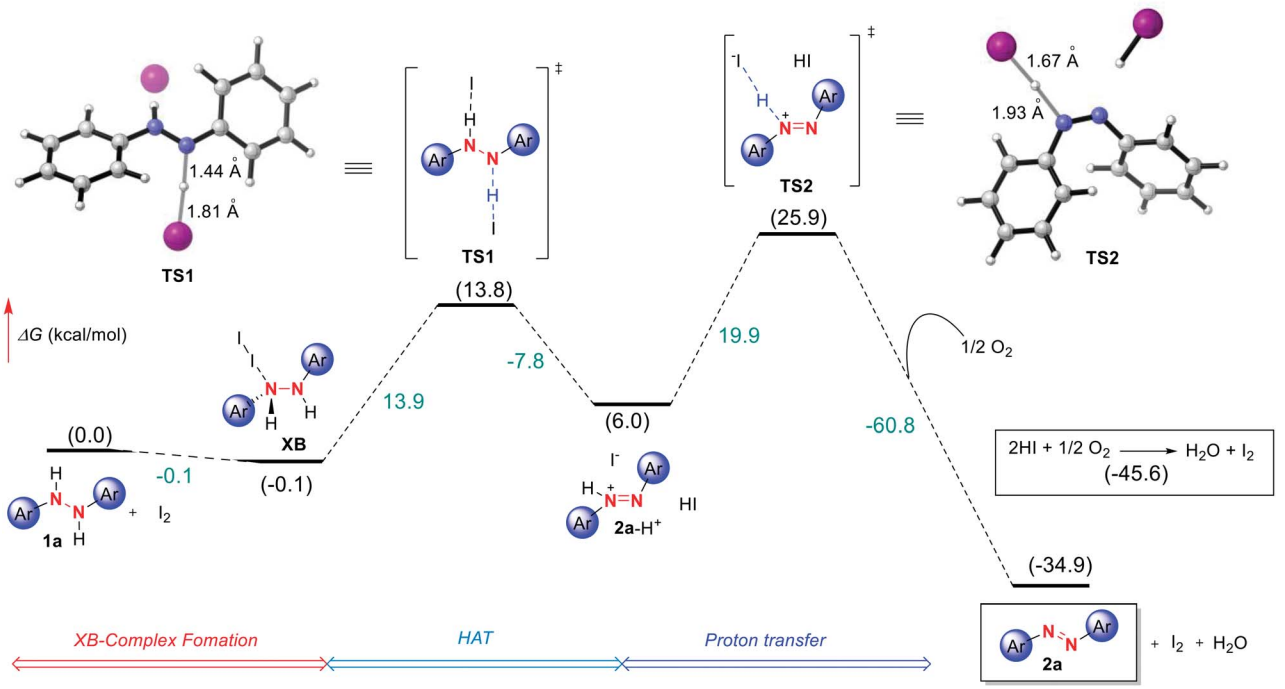

Fig. 3 Free energy profile for I_2 catalyzed azo formation computed at the (IEFPCM$_{DCM}$)UAPFD/def2-TZVP//UAPFD/DGDZVP level of theory. Free energies are given in kcal mol^{-1}.

determining intermediate (TDI), while the TOF determining transition state (TDTS) is **TS2**, thus resulting in an overall energy span of 26.0 kcal mol^{-1} (TON = 5.5 × 10^{-8}, TOF = 2.9 × 10^{-9} s^{-1}).[29]

Greenness measurements of the procedure

Lastly, to highlight the overall *greenness* and efficiency of our molecular iodine catalyzed azo forming protocol we employ green metrics.[30] In this regard, as no one green metric is capable of accounting for every possible parameter influencing the environmental impact of a process, we use several green metrics and the standard reaction metric yield for this analysis. Further, to showcase the favorability of our protocol comparisons are made to previous literature reports for oxidizing hydrazine HN–NH bonds to azo groups. For this analysis two metrics relating to mass efficiency were selected; (1) Sheldon's *E*-factor was selected as an easy measure of relative waste and (2) GlaxoSmith-Klein's (GSK) metric was used to gauge reaction mass efficiency. Carbon efficiency (CE) was also calculated to determine the efficiency of the transfer of organic material. *E*-Factors and RME were calculated by eqn (1) and (2) respectively, such that m_{sm} is the mass of starting materials and m_p is the mass products.[31]

$$E = \frac{m_{sm} - m_p}{m_p} \quad (1)$$

$$\mathrm{RME} = \frac{m_p}{m_{sm}} \times 100 \quad (2)$$

The mass of all consumable starting reagents and catalysts were incorporated, while solvents and silica gel were considered recoverable and aqueous solutions were considered benign, and therefore excluded from the calculation. These assumptions were made for the sake of comparing bench scale chemistries, where solvent choices, quantities and lifecycles can be expected to change significantly during scale-up to an industrial process. CE was determined according to eqn (3), such that n_p is the moles of product, n_{sm} is the moles of each reagent, C_{sm} is the number of carbons of that reagent and C_p is the number of carbons in the product.

$$\mathrm{CE} = \frac{n_p \times C_p}{\sum C_{sm} \times n_{sm}} \times 100\% \quad (3)$$

Overall, the green metrics and yield of our reaction are high, if not, excellent as seen from Table 4. This is clearly seen by comparison with reported *t*-BuOCl and *t*-BuOK procedures for oxidizing hydrazine HN–NH bonds to azo groups.[17,32] In terms of yield and Reaction Mass Efficiency (RME) all three procedures are high yielding with respectable RME values. Though the reported quantitative isolated product yield for the dehydrohalogenation procedure of Okumura *et al.*[17] is remarkable given the need for several purification steps, including silica gel flash chromatography. Meanwhile, our iodine-catalyzed oxidation procedure benefited from significantly higher carbon efficiency (CE) compare to the two other reported procedures, in addition to having a much lower *E*-factor making it a greener chemistry.

Finally, in speaking to sustainability and in light of the new twelve green chemistry principles promulgated recently by Zimmerman *et al.*,[33] it is notably our reported molecule iodine catalyzed synthesis of azo compounds fulfils the majority of these twelve principles.

Table 4 Comparison of oxidation reaction metrics and primary oxidants of diphenylhydrazine

Metric	Okumura *et al.*[17]	Wang *et al.*[32]	This work
Yield of **2a**	100%	97%	98%
Oxidant	*t*-BuCl (2 equiv.)	*t*-BuOK (40 mol%)	I_2 (2 mol%)
E-Factor	2.67	0.93	0.06
RME	99%	95%	95%
CE	60%	85.6%	98%

Conclusion

To recap, in harnessing the oxidative power of molecular iodine, we have reported an innovative catalytic method for converting hydrazine HN–NH bonds to azo group N=N double bond functionally. The significance of this work is manifold, including the use of commercially available, cheap, and easy-to-handle molecular iodine as a non-metal catalyst. In addition, the synthetic protocol described in this letter allows for the preparation of privileged azo group functionality from plentiful hydrazine precursors, while offering underlying mechanistic understanding into iodine catalysis. Ongoing efforts in our lab are expanding this unique reactivity to a repertoire of uses and related findings will be reported in due course.

Conflicts of interest

There are no conflicts to declare.

Acknowledgements

T. D. acknowledges financial support from the Natural Science and Engineering Research Council (NSERC) Discovery grant (2019-04205). Computations were carried out using facilities at SHARCNET (Shared Hierarchical Academic Research Computing Network: http://www.sharcnet.ca) and Compute/Calcul Canada. T. D. and R. R. thank the "Brock Library Open Access Publishing Fund".

References

1 S. V. Heins, *J. Chem. Educ.*, 1958, **35**, 187.
2 R. G. Anderson and G. Nickless, *Analyst*, 1967, **92**, 207.
3 (*a*) L. Androvic, J. Bartacek and M. Sedlak, *Res. Chem. Intermed.*, 2016, **42**, 5133; (*b*) D. Braun, *Int. J. Polym. Sci.*, 2009, **2009**, 1.
4 N. A. Naser, K. H. Kahdim and D. N. Taha, *J. Oleo Sci.*, 2012, **61**, 387.
5 N. DiCesare and J. R. Lakowicz, *Org. Lett.*, 2001, **3**, 3891.
6 H. K. Bisoyi and Q. Li, *Chem. Rev.*, 2016, **116**, 15089.
7 S. Xie, A. Natansohn and P. Rochon, *Chem. Mater.*, 1993, **5**, 403.

8 M. A. Kienzler and E. Y. Isacoff, *Curr. Opin. Neurobiol.*, 2017, **45**, 202.
9 (*a*) S. Kadota, K. Aoki, S. Nagano and T. Seki, *J. Am. Chem. Soc.*, 2005, **127**, 8266; (*b*) Y. Zhao and J. He, *Soft Matter*, 2009, **5**, 2686.
10 S. Okumura, Y. Takeda and S. Minakata, *Angew. Chem.*, 2012, **124**, 7924.
11 (*a*) L. Hu, X. Cao, L. Shi, F. Qi, Z. Guo, J. Lu and H. Gu, *Org. Lett.*, 2011, **13**, 5640; (*b*) N. Sakai, K. Fujii, S. Nabeshima, R. Ikeda and T. Konakahara, *Chem. Commun.*, 2010, **46**, 3173.
12 J. H. Boyer, in *The Chemistry of the Nitro and Nitroso Groups, Part 1*, ed. H. Feuer, Interscience, New York, 1969, pp. 278–283.
13 (*a*) H. A. Dabbagh, A. Teimouri and A. N. Chermahini, *Dyes Pigm.*, 2007, **73**, 239; (*b*) M. Barbero, S. Cadamuro, S. Dughera and C. Giaveno, *Eur. J. Org. Chem.*, 2006, **21**, 4884; (*c*) K. Haghbeena and E. W. Tan, *J. Org. Chem.*, 1998, **63**, 4503.
14 (*a*) Y. Zhu and Y. Shi, *Org. Lett.*, 2013, **15**, 1942; (*b*) Z. Hu and F. M. Kerton, *Org. Biomol. Chem.*, 2012, **10**, 1618; (*c*) W. Lu and C. Xi, *Tetrahedron Lett.*, 2008, **49**, 4011.
15 B. Ortiz, P. Villanueva and F. Walls, *J. Org. Chem.*, 1972, **37**, 2748.
16 (*a*) H. Firouzabadi, D. Mohajer and M. Entezari-Moghadam, *Bull. Chem. Soc. Jpn.*, 1988, **61**, 2185; (*b*) H. Huang, D. Sommerfeld, B. C. Dunn, C. R. Lloyd and E. M. Eyring, *J. Chem. Soc., Dalton Trans.*, 2001, **8**, 1301.
17 S. Okumura, C. H. Lin, Y. Takeda and S. Minakata, *J. Org. Chem.*, 2013, **78**, 12090.
18 H. Firouzabadi and Z. Mostafavipoor, *Bull. Chem. Soc. Jpn.*, 1983, **56**, 914.
19 E. Baer and A. L. Tosoni, *J. Am. Chem. Soc.*, 1956, **78**, 2857.
20 (*a*) S. Farhadi, P. Zaringhadam and R. Z. Sahamieh, *Acta Chim. Slov.*, 2007, **54**, 647; (*b*) K. Orito, T. Hatakeyama, M. Takeo, S. Uchiito, M. Tokuda and H. Suginome, *Tetrahedron*, 1998, **54**, 8403.
21 (*a*) G. Jurmann, O. Tsubrik, K. Tammeveski and U. Maeorg, *J. Chem. Res.*, 2005, **2005**, 661; (*b*) M. J. S. Dewar, *J. Chem. Soc.*, 1946, **160**, 777; (*c*) W. Wang, G. Tan, R. Feng, Y. Fang, C. Vhen, H. Ruan, Y. Zhao and X. Wang, *Chem. Commun.*, 2020, **56**, 3285.
22 (*a*) H. Lv, R. D. Laishram, Y. Yang, J. Li, D. Xu, Y. Zhan, Y. Luo, Z. Su, S. More and B. Fan, *Org. Biomol. Chem.*, 2020, **18**, 3471; (*b*) G. Jo, M. H. Kim and J. Kim, *J. Org. Chem.*, 2020, **7**, 834; (*c*) Y. Xu, X. Shi and L. Wu, *RSC Adv.*, 2019, **9**, 24025.
23 (*a*) P. P. Power, *Nature*, 2010, **463**, 171; (*b*) T. A. Engesser, M. R. Lichtenthaler, M. Schleep and I. Krossing, *Chem. Soc. Rev.*, 2016, **45**, 789; (*c*) R. L. Melen, *Science*, 2019, **363**, 479; (*d*) J. R. Lawson and R. L. Melen, *Inorg. Chem.*, 2017, **56**, 8627.
24 G. R. Desiraju, P. S. Ho, L. Kloo, A. C. Legon, R. Marquardt, P. Metrangolo, P. Politzer, G. Resnati and K. Rissanen, *Pure Appl. Chem.*, 2013, **85**, 1711.
25 (*a*) T. Clark, M. Hennemann, J. S. Murray and P. Politzer, *J. Mol. Model.*, 2007, **13**, 291; (*b*) P. Politzer, J. S. Murray and T. Clark, *Phys. Chem. Chem. Phys.*, 2013, **15**, 11178.
26 (*a*) M. Colin and H. Gaultier de Claubry, *Ann. Chim.*, 1814, **90**, 87; (*b*) M. Colin, *Ann. Chim.*, 1814, **91**, 252.
27 (*a*) D. S. Barak, S. U. Dighe, I. Avasthi and S. Batra, *J. Org. Chem.*, 2018, **83**, 3537; (*b*) O. Prakash, H. K. Gujral, N. Rani and S. P. Syn, *Com*, 2000, **30**, 417; (*c*) H. Liu, Y. Wei and C. Cai, *New J. Chem.*, 2016, **40**, 674.
28 Recently, Fan *et al.* reported the use of TEMPO as an organocatalyst for the oxidative dehydrogenation of hydrazobenzenes to azobenzenes, see ref. 22*a* (*vide supra*). Notably, compared to this reported procedure our I_2 catalyzed protocol has the advantages of using lower catalyst loadings and much shorter reaction times, in addition to not requiring heating.
29 (*a*) S. A. Kozuch, *Comput. Mol. Biosci.*, 2012, **2**, 795; (*b*) S. Kozuch and S. Shaik, *Acc. Chem. Res.*, 2011, **44**, 101; (*c*) A. Uhe, S. Kozuch and S. Shaik, *J. Comput. Chem.*, 2011, **32**, 978.
30 (*a*) R. A. Sheldon, *Chem. Commun.*, 2008, 3352; (*b*) R. A. Sheldon, *Green Chem.*, 2007, **9**, 1273; (*c*) For a recent comparison of 'Green' metrics see: D. J. C. Constable, A. D. Curzons and V. L. Cunningham, *Green Chem.*, 2002, **4**, 521; (*d*) For other 'Green' metrics see: T. Hudlicky, D. A. Frey, L. Koroniak, C. D. Claeboe and L. E. Brammer, *Green Chem.*, 1999, 57; (*e*) B. M. Trost, *Science*, 1991, **254**, 1471; (*f*) A. D. Curzons, D. J. C. Constable, D. N. Mortimer and V. L. Cunningham, *Green Chem.*, 2001, **3**, 1.
31 P. T. Anastas and J. C. Warner, *Green Chemistry: Theory and Practice*, Oxford University Press, New York, 1998, p. 30.
32 L. Wang, A. Ishida, Y. Hashidoka and M. Hashimoto, *Angew. Chem., Int. Ed.*, 2017, **56**, 870.
33 J. B. Zimmerman, P. T. Anastas, H. C. Erythropel and W. Leitner, *Science*, 2020, **367**, 397.